Anal Bioanal Chem (2014) 406:183–192
DOI 10.1007/s00216-013-7437-5

RESEARCH PAPER

Differentiation of *Escherichia coli* serotypes using DC gradient insulator dielectrophoresis

Paul V. Jones · Alexa F. DeMichele · LaKeta Kemp · Mark A. Hayes

Received: 10 July 2013 / Revised: 8 October 2013 / Accepted: 14 October 2013 / Published online: 8 November 2013

Abstract Bacteria play a significant role in both human health and disease. An estimated 9.4 million cases of foodborne illness occur in the United States each year. As a result, rapid identification and characterization of microorganisms remains an important research objective. Despite limitations, selective culturing retains a central role among a cadre of identification strategies. For the past decade, separations-based approaches to rapid bacterial identification have been under investigation. Gradient insulator dielectrophoresis (g-iDEP) promises benefits in the form of rapid and specific separation of very similar bacteria, including serotypes of a single species. Furthermore, this approach allows simultaneous concentration of analyte, facilitating detection and downstream analysis. Differentiation of three serotypes or strains of *Escherichia coli* bacteria is demonstrated within a single g-iDEP microchannel, based on their characteristic electrokinetic properties. Whole cells were captured and concentrated using a range of applied potentials, which generated average electric fields between 160 and 470 V/cm. Bacteria remained viable after exposure to these fields, as determined by cellular motility. These results indicate the potential g-iDEP holds in terms of both separatory power and the possibility for diagnostic applications.

Keywords Dielectrophoresis · *Escherichia coli* · Bioanalytical methods · Electrokinetic separations · Microfluidics

P. V. Jones · A. F. DeMichele · L. Kemp · M. A. Hayes (✉)
Department of Chemistry and Biochemistry, Arizona State University, Tempe 85287-1604, AZ, USA
e-mail: MHayes@asu.edu

Abbreviations

DC	Direct current
DEP	Dielectrophoresis
EOF	Electroosmotic flow
EP	Electrophoresis
g-iDEP	Gradient-insulator-based dielectrophoresis
iDEP	Insulator dielectrophoresis

Introduction

It is believed that over 10^{30} bacteria live on planet Earth and their biomass may exceed that of all other organisms combined [1]. The average human intestine is home to about 10^{14} bacteria—a microbiome composed of 500–1,000 individual species [2]. Bacteria in the environment, of course, represent an even more complex array of species and niches. Typically, these organisms are commensal or mutualistic, conferring some benefit to each other or their host. Some species, however, are pathogenic. Most strains of *Escherichia coli*, for instance, are innocuous to humans. However, as recent headlines note, some can cause intoxication and infection where resulting syndromes may lead to death.

Relatively little is known about the immense diversity of species comprising the gut flora that crowds the human intestine. Many species remain unknown since most identification strategies require culturing—the growth of particular species in artificial environments—and many species will not accommodate this strategy. False negatives have been documented to reach at least 70 % when conventional microbiological culture is used alone [3–5].

In practical settings, bacteria are identified by molecular biologists and microbiologists, who use an ensemble of tests

to accomplish this task. Species and strains are identified and grouped by phenotypic characteristics such as appearance and immunologic reactivity, and genotypic characteristics. Specific examples of tests used for classification include differential staining, selective culturing, serological typing, nucleotide sequence recognition, and flow cytometry [6]. Many of these methods require preparation and growth of cultures, which significantly extends the time required for analysis. Culturing also reduces the possibility of determining the abundance or population diversity of microbes in the original sample. While nucleic acid amplification methods minimize or eliminate the need for culturing, DNA isolation and purification can be laborious. Emerging commercial approaches involving rapid PCR may reduce the time and preparation required for such tests, but involve benchtop instruments, only detect previously identified targets for which sequences are established, and typically only screen for panels of very common pathogens. As such, these approaches do not lend themselves to the development of rapid and broad field-based analysis [7].

A separations-based strategy for isolating and concentrating intact microorganisms could offer significant benefits over traditional approaches. Rapid identification and quantitation could provide revolutionary benefits in scientific, clinical, and environmental applications. A number of scientists, for over 50 years, have recognized that different cells have unique electrical properties and furthermore that those properties can be detected and used to initiate separations between different types of cells. Early work focused on sensing unique resistive and dielectric properties via impedance spectroscopy. These works often investigated the electric properties of single species by applying an alternating potential across the cells and recording current with respect to frequency [8–10]. Others attempted to bifurcate samples into two analyte populations (e.g., leukemic cells and erythrocytes) [11–14]. This research defined many unique and quantifiable differences between bacteria and many other types of cells.

A number of researchers have pursued capillary electrophoresis (CE) of microorganisms [15]. However, designing such a separation scheme faces many hurdles. As targets for analytical separations, bacteria and other microbes are both attractive and uniquely challenging. After several years developing novel approaches to CE of bacteria, Armstrong et al. identified a few of the chief difficulties involved with bacterial CE separations. These include long separation times, poor specificity, sensitivity of the analyte to the surrounding analytical environment, requirements for sample purity, and microbe aggregation [16]. CE separations of bacteria have yielded interesting results, but are typically plagued by band broadening. This decreases selectivity and separation efficiency. Armstrong et al. introduced the use of poly(ethylene oxide) (PEO) as a dynamic additive in bacterial separations. This dramatically increased apparent separation efficiency; however, peak purity was not assessed and the narrow peaks were determined to result from microbial aggregation.

Innovations using mass spectrometry (MS) provide an interesting alternative route to microbe identification. MS is typically used to identify small and large molecules. Identification of cells involves breaking them into ionized molecular fragments and measuring mass/charge ratio of the products. Cells can be identified by the characteristic fingerprint they produce in such analyses. Mass spectrometry faces many challenges, however, including the need for sample purity, broad chemical differences in cell species, and variations between stages of cell development.

Recent electrokinetic (EK) approaches to the manipulation and analysis of microbes and other cells have demonstrated the potential for significant improvements over traditional methods. Dielectrophoresis (DEP) offers tantalizing benefits in the form of extremely rapid and specific separations that can occur while simultaneously concentrating the analyte. Dielectrophoretic force results from the interaction between permanent or field-induced dipoles and a spatially inhomogeneous electric field. DEP acts upon analyte in concert with other field-induced forces such as electrophoresis (EP) and electroosmotic flow (EOF). Together, these three forces provide multiple force vectors with which to query a variety of analyte properties, including but not limited to particle size, structure, surface charge, charge heterogeneity, polarizability, and permittivity differences between the cells and the buffer. These traits can vary widely between cells and microbes that otherwise appear and behave similarly. As one example, DEP has been used to differentiate erythrocytes based on antigen expression [17].

Early implementations of DEP used patterned electrodes to generate AC field gradients. Separations were based on the characteristic crossover frequency, where net dielectrophoretic force switches from positive (up-gradient) to negative (down-gradient). Later work used electrically insulating structures to impinge upon field lines and induce a local gradient. Beginning in 2002, this work was rapidly expanded [18, 19]. The use of insulator-based dielectrophoresis (iDEP) ameliorated many of the problems associated with traditional DEP experiments, which included electrolysis within separation zones, Joule heating, cellular damage, and complex fabrication procedures. DC iDEP also enabled the simultaneous use of field-driven flow through separation zones.

The work presented here utilizes an approach to iDEP first introduced in 2007, in which insulating sawtooth features along the sides of a microchannel create electric field inhomogeneities [20]. Progressive changes in the tooth geometry create distinct zones of increasing local field gradient along the length of the channel. This progression of

local maxima yields a secondary macro-gradient globally across the device. Analyte is driven through the channel by a combination of EP and EOF. Particles traveling down the channel encounter zones of increasing DEP force as they approach each set of opposing teeth. When DEP force is sufficient to counter the combination of EP and EOF, particles are trapped and prevented from further translation down the channel. This causes particles to stop at discrete and unique points along the channel based on their individualized electrokinetic properties.

Using this approach, our group is refining the separation of bacterial species and strains based on their physical and electrical properties. The work presented here is unique for three reasons. First, it uses a linear separation mode combining electrophoresis, electroosmotic flow, and dielectrophoresis, where a distinctive balance point can be found for an analyte based on the ratio of its electrokinetic mobility (the sum of electrophoretic and electroosmotic mobilities) and dielectrophoretic mobility. Second, it is an extremely high-resolution separation scheme, better than many traditional electrophoretic and dielectrophoretic strategies. Third, we demonstrate that individual strains of *E. coli* can be differentiated. This suggests an opportunity to begin to identify bacteria by their electric properties. Specifically, this work indicates that three serotypes of *E. coli* can be differentiated within an appropriately designed g-iDEP microchannel, including differentiation of pathogenic from non-pathogenic types.

Materials and methods

Microdevice fabrication

The geometry of the sawtooth channel has been described previously. In brief, it consists of adjoined triangular units aligned along each side of a channel (Fig. 1). Successive narrowed segments are formed where the tips of each set of opposing triangles draw together. These narrowed regions are considered gates for this discussion. The equilateral, triangular units increase in size along the length of the channel, causing the apices of opposing triangles or teeth to gradually converge towards the channel centerline. For this particular case, the channel length, width, and depth were 4.1 cm, 1,000 μm, and 14±1 μm (average between templates), respectively. The initial gate width was 945 μm and the final one 27 μm.

The microfluidic devices used in these experiments were fabricated using soft lithography [21, 22]. The sawtooth channels were patterned on 4-in. Si wafers using AZ P4620 positive photoresist (AZ Electronic Materials, Branchburg, NJ) and contrast enhancement material CEM388SS (Shin-Etsu MicroSi, Inc., Phoenix, AZ). The photoresist was exposed with a high-fidelity chrome photomask, and then developed. Polydimethylsiloxane (PDMS) (Sylgard 184, Dow/Corning, Midland, MI) was poured over the resulting templates and allowed to cure at 70 °C for 1 h. PDMS casts were then peeled from the template wafers, trimmed to size, and punched with 2-mm-diameter holes for access to the round, terminal reservoirs at each end of the channel.

Finalized devices were constructed from PDMS casts bonded to a glass coverplate. This approach yielded microfluidic channels with three walls of PDMS and one of glass. The two materials were treated with oxygen plasma in a Tegal asher (PlasmaLine 411; Tegal Corporation, Petaluma, CA) and then allowed to seal upon contact.

Cell culture and labeling

Three strains of *E. coli* were obtained including serotypes O157:H7, strain 465-97; O55-H7; and a quality control strain O6:K1:H1, equivalent to ATCC 25922. Each strain represents a different serogroup and will be referred to by serotype only.

E. coli seed stock was stored on biobeads in Brucella Broth with 10 % glycerol at −80 °C. Ten-milliliter aliquots of sterile lysogeny broth (LB) (Sigma-Aldrich Co., St. Louis, MO) were placed in culture tubes. Each tube was inoculated with one of the strains then incubated overnight at 37 °C. This allowed each culture to reach late log phase, with a cell concentration of approximately 10^9 cells/mL. Following incubation, 500-μL aliquots of each cell culture were centrifuged at 4,000×*g* for 3 min. The supernatant was discarded and the cell pellet resuspended by adding 1 mL 2 mM phosphate buffer at a pH of 7.4 and mixing with a vortexer for 10–15 s. This process was repeated two more times in order to wash the cells and remove the LB broth.

Cells were labeled using Vybrant DiO fluorescent dye (Invitrogen) [23–25]. Excitation and emission wavelengths for this dye are 484 and 501 nm, respectively. A 5-μL aliquot of dye was added to each 1-mL suspension of washed cells. These were incubated in a 37 °C water bath for approximately 20 min. The samples were then washed three times in order to eliminate free dye. This was accomplished by centrifuging and resuspending the cells in phosphate buffer as described above, with the exception that the final buffer solution contained 4 mg/mL bovine serum albumin (BSA). Throughout the labeling process, exposure to ambient light was minimized in order to prevent photobleaching. Examination of the dispersed, suspended cells using a microscope revealed that they were individual, intact cells, with minimal aggregation.

Experimental

The microdevice was placed on the stage of an Olympus IX70 inverted microscope with a ×4 or ×10 objective for

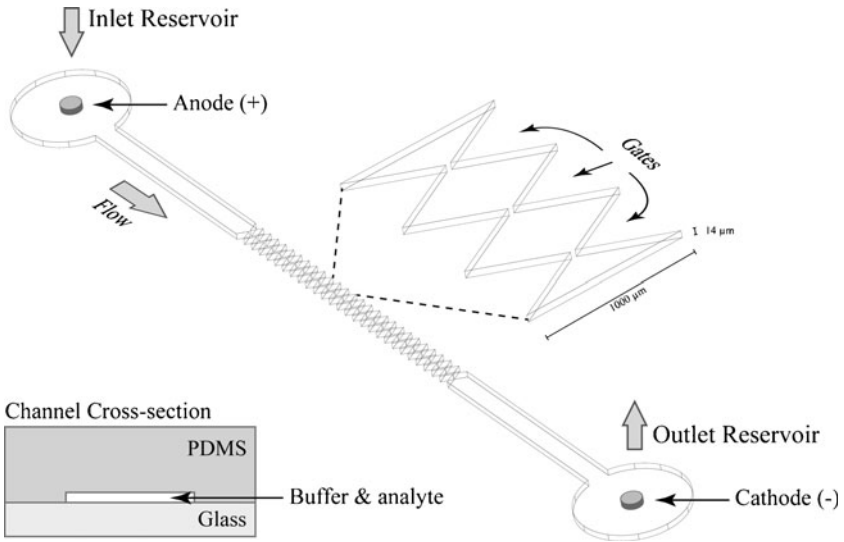

Fig. 1 Schematic diagram of a g-iDEP microchannel. For these experiments, devices were constructed of glass and PDMS

observation and data collection. Samples were introduced into the microdevice by pipetting ~20 μL of cell suspension into the inlet reservoir. Hydrodynamic flow was balanced by pipetting a similar volume of buffer into the outlet reservoir. Particle motion within the channel was observed in order to monitor and ensure stasis of flow. A mercury short arc lamp (H30 102 w/2, OSRAM) was used for illumination. An Olympus DAPI, FITC, Texas Red triple band-pass cube (Olympus, Center Valley, PA) was used for fluorescence microscopy. Both still images and video were collected with a monochrome QICAM cooled CCD camera (QImaging, Inc., Surrey, BC) and Streampix V image capture software (Norpix, Inc., Montreal, QC).

Platinum electrodes with a diameter of 0.404 mm (Alfa Aesar, Ward Hill, MA) were inserted through the PDMS access ports into the terminal reservoirs. They were then connected to a HVS448 3000D high voltage sequencer (Labsmith, Inc., Livermore, CA).

Bacteria were captured in both deionized H_2O (DI-H_2O) and 2 mM phosphate buffer at a pH of 7.4. The conductivities of these solutions were 55.3 and 343 μS/cm, respectively. DI-H_2O and buffer solutions also contained BSA ranging in concentration from 0 to 8 mg/mL. The experiments described here contained BSA at 4 mg/mL. DC potentials applied across the device ranged from 0 to 3,000 V in 100-V increments. These potentials correspond to average field strengths (E_{app}= V/4.1 cm) of 0–732 V/cm and increments of approximately 24 V/cm.

Particle image velocimetry measurements were used to determine the EK velocity of the bacteria. Cell motion was observed within the straight portions of the microchannel proximal to each reservoir. Local electric field strength was determined using COMSOL Multiphysics modeling. These values were used along with velocity data to estimate EK mobilities.

Mathematical modeling

Electric field characteristics in the microchannel were numerically modeled with COMSOL Multiphysics software (COMSOL, Inc., Burlington, MA). The model consisted of a properly scaled 2D geometry of the main channel, excluding the device reservoirs. A 2D approximation greatly simplifies the calculations and was used since the electrical potential is presumed to vary minimally across the relatively small depth of the microchannel. The conductivity and relative permittivity of the medium were set to 1.2 S/m and 78, respectively.

Safety considerations

Organisms used in this experiment were Biosafety Level I or II. All experiments were carried out in an approved BSL II laboratory within accordance with the current version of the CDC/NIH BMBL publication.

Results

Three strains of *E. coli*, expressing O157:H7, O55:H7, or O6:K1:H1 antigenic phenotypes, with each being a different serotype, were investigated within g-iDEP devices. Their behavior was examined primarily at the final three sets of gates within the microchannel, namely those with a gate pitch of 300, 90, or 27 μm. Gate pitch refers to the distance between the points of opposing teeth. The magnitude of the electric potential applied across the device was recorded in terms of ΔV divided by 4.1 cm, the overall length of the channel, designated E_{app}. The value of E_{app} was varied along with the duration of applied potential (t_{app}). The location of collection was noted in terms of gate pitch.

Electrokinetic and dielectrophoretic behaviors of the bacteria were broadly consistent with prior observations of other samples in g-iDEP devices. Upon application of potential, bulk motion of particles was initiated towards the outlet reservoir, which housed the cathode, consistent with expected EOF direction and charge state of bacteria [26]. No particle capture was observed in the wide-gated segments of the sawtooth channel (gate pitch >300 μm). Within these regions, all visible material traveled consistently towards the cathode in the outlet reservoir. Capture resulted in the formation of crescent-shaped bands of concentrated particles immediately upstream of a given gate (Fig. 2) [20, 22, 27, 28]. Unique capture and concentration of all three *E. coli* serotypes was observed.

All three serotypes were captured at 27 μm gates, with statistically significant differences in E_{app} required for capture of each. Only two serotypes were captured at 90 μm gates, and one serotype at 300 μm gates. The behavior of O6:K1:H1 and O55:H7 indicates that the difference in E_{app} required for capture of different serotypes increases at larger gate pitches.

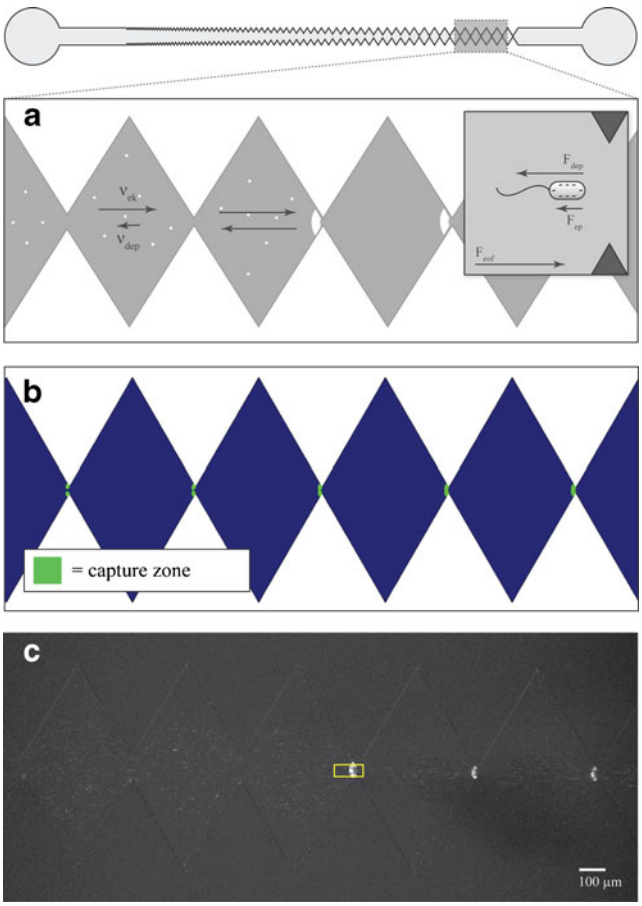

Fig. 2 **a** Illustration showing capture of *E. coli* organisms as predicted by the presence of opposing electrokinetic and dielectrophoretic forces. **b** Capture zones modeled using COMSOL Multiphysics. **c** Image showing capture of fluorescently labeled bacteria. The *yellow box* indicates the region of interest used for fluorescence intensity measurement

The amount of material captured at a particular gate was dependent upon the magnitude and duration of the applied electric field. Below a particular value of E_{app}, no capture occurred, even over extended periods of time. That threshold value is referred to as E_{onset} and occurred after sufficient potential was applied across the device, causing particles to collect in characteristic zones near the entrance to a gate. Capture was monitored by local fluorescence intensity. Material continued to capture while potential was applied. Since collection varied with both t_{app} and E_{app}, data was collected and compared at consistent time points following application of the electric field. By holding t_{app} constant, the dependence of capture on E_{app} could be investigated. Above E_{onset}, the rate of particle accumulation increased with E_{app} (Fig. 3). This was observed both via qualitative image analysis and fluorescence intensity measurements.

Integrated fluorescence intensity (FI) was measured within a small region of interest at expected capture zones. Plots of these data corresponded with qualitative observations. Specifically, measured values of FI increased rapidly with t_{app} above E_{onset} (Fig. 4a). FI measurements were taken at t_{app}=5 s and plotted versus E_{app}, elucidating characteristic behaviors for each serotype at the various gate pitches. At values of E_{app} greater than E_{onset}, FI continued to increase before eventually leveling off. This yielded plots with a roughly sigmoidal shape (Fig. 4b).

Repeated experiments demonstrated a similar behavior. Figure 5 shows the average integrated fluorescence intensity for data collected from five different devices with separate bacterial preparations of serotype O6:K1:H1. Error bars indicate the standard deviation of each set.

The inflection points of the sigmoidal curves shown in Fig. 4b were used as the serotype-specific E_{onset} values for appreciable capture. These E_{onset} values were plotted versus gate pitch for each serotype (Fig. 6). E_{onset} values for O6:K1:H1 were 163±31, 259±52, and 427±53 V/cm for the 27-, 90-, and 300-μm gates, respectively. E_{onset} values for O55:H7 were 290±16 and 470±8 V/cm at 27- and 90-μm gates. For O157:H7, E_{onset} was 324±25 V/cm at 27-μm gates. The results indicate statistically significant differences in capture behavior for the three serotypes of *E. coli* bacteria.

Unstained samples of each *E. coli* serotype were also used on microdevices and observed using a combination of brightfield and darkfield microscopy. Capture data from these runs agreed identically with that obtained using fluorescently labeled samples, suggesting that the electrokinetic effects of the membrane-intercalating dye were negligible within the framework of this application.

Discussion

In order to understand behavior of these species in a g-iDEP microchannel, it is instructive to briefly consider their

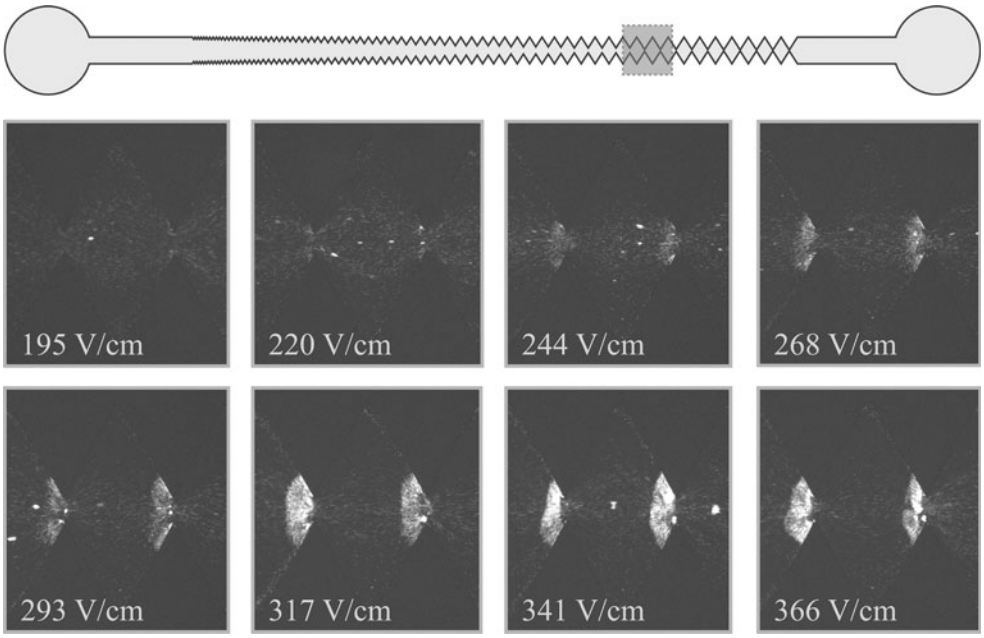

Fig. 3 Capture of O6:K1:H1 at 90-μm gates. In each image, t_{app}=5 s. Capture only occurs above a threshold value of E_{app}

physicochemical characteristics. The cell surface of gram-negative bacteria such as *E. coli* typically consists of various phospholipids, membrane proteins, and a LPS coat [29]. The lipopolysaccharide layer on the outer leaflet of the *E. coli* membrane (associated with the O antigen) is expected to contribute significantly to negative surface charge due to the presence of both carboxylic acid and phosphate moieties [30]. Large-scale surface features such as flagella and fimbriae also affect the cell's surface properties [31]. Various strains of *E. coli* differ in their biochemical and physical phenotypes. Distinctions between strains can manifest in terms of protein expression, glycosylation, LPS structure, as well as differences in their flagella, fimbriae, and internal structures [32]. Considered together, these phenotypic differences can impact the charge and polarizability of *E. coli* cells, and thus contribute to different electrophoretic and dielectrophoretic mobilities.

Utilizing g-iDEP methodology presents unique opportunities to exploit these differences to generate separations. Although the complexity of biological objects like bacterial cells creates unique challenges, it also furnishes a rich set of vectors for separatory differentiation. Demonstrations of bioparticle capture using this approach have shown rapid, specific capture from heterogeneous samples.

For the purposes of this discussion, EK motion refers to the transport of particles induced by the application of an external electric field. In these experiments, EK transport included the effects of EP and EOF, which are both directly proportional to electric field strength. In the case of small particles, EP force is proportional to net surface charge as well as field strength. At or below neutral pH, *E. coli* bacteria possess a negative surface charge. As such, EP force will be directed toward positive electric potential. Above a pH of ~4, glass and oxidized PDMS surfaces carry a negative surface charge. This produces EOF in the opposite direction or towards negative electric potential. In these experiments, pH was maintained at 7.4. As a result, the observed motion of all bacteria towards the negative electrode indicated that under these conditions the electroosmotic mobility (μ_{EO}) exceeded the electrophoretic mobility (μ_{EP}) of the bacteria. Although dominant μ_{EO} determined the direction of transport, differences in μ_{EP} between analytes still contribute significantly to net electrokinetic mobility (μ_{EK}) and the resulting translational velocity of particles.

Electrophoretic mobilities for various serotypes of *E. coli*, including O157:H7, have been reported in the range of -0.2×10^{-4} to -1.4×10^{-4} cm^2/V s at or near neutral pH [33]. However, these values vary with buffer pH and ionic strength. Within the g-iDEP microchannel, μ_{EP} was not measured directly. Instead, an effective estimated μ_{EK} was determined via particle tracking. Positive values support that EOF exceeded EP force. Values of μ_{EK} determined for *E. coli* in the g-iDEP microchannel ranged from 1.2×10^{-4} to 2.5×10^{-4} cm^2/V s.

Theoretical descriptions of dielectrophoretic behaviors of cells utilize multishell models to approximate cell structure and heterogeneity [34]. In these models, cells are treated as bodies consisting of onion-like layers with varying electrical properties. *E. coli* can be approximated as a prolate ellipsoid, with two finite-thickness shells encapsulating the cytoplasm. The outer and inner shells represent the LPS layer and cell membrane, respectively. The cytoplasm and each shell are attributed unique values for permittivity and conductivity.

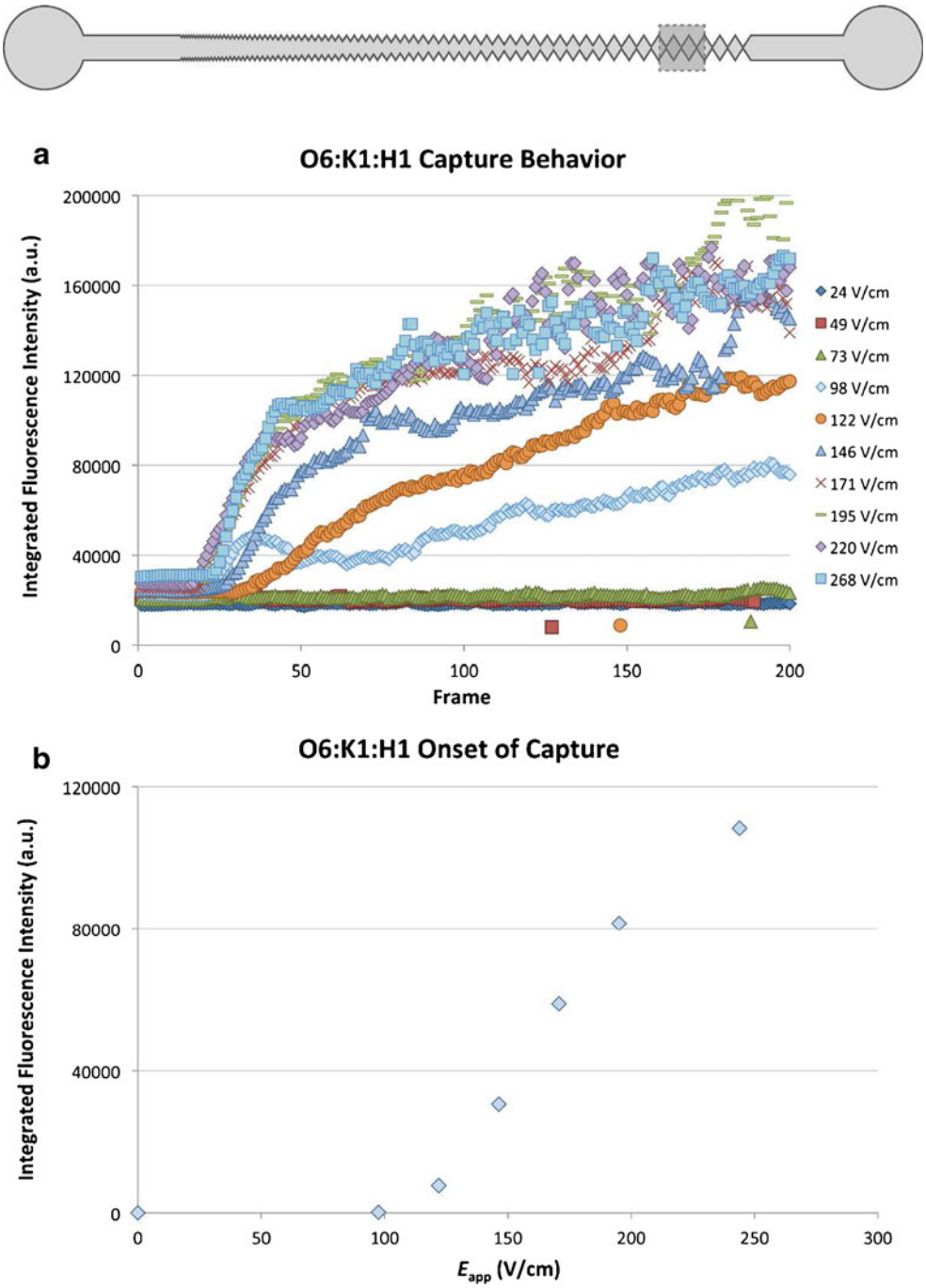

Fig. 4 Plots showing fluorescence intensity data for capture of O6:K1:H1. **a** Plot showing the accumulation of material over time for various applied field strengths. No capture occurs when E_{app} is 100 V/cm or less, even over extended periods of time. Above this range, capture is observed almost immediately. 120 to 200 V/cm comprise a transition zone, where capture begins to occur, but is not completely exclusive. Above 200 V/cm, increasing the applied field strength does not appreciably affect the accumulation of material with time. **b** Plot showing fluorescence intensity increase at a capture zone (gate) versus applied field strength. Each FI measurement was taken after 5 s of applied potential

These models indicate that at low frequencies, including DC fields, the conductivity of the LPS layer (σ_{wall}) and cell membrane (σ_{mem}) factor significantly into the dielectric properties of the cell [35]. The dielectric properties of bacteria have yet to be precisely characterized. No alternative or independent quantitative information exists for both size and dielectric differences between strains of *E. coli*. Work performed by Castellarnau et al. using AC DEP focused on crossover frequencies of isogenic mutants of one strain of *E. coli* and further utilized a multishell model to estimate conductivities of cell cytoplasm, membrane, and wall [35]. The geometric parameters used for these calculations involved an ellipsoid with axes $a=3/2$ and $b=a/2$, cell membrane thickness of 8 nm, and cell wall thickness of 50 nm. Using this approach, respective values for σ_{wall} and σ_{mem} were estimated to be 58×10^{-3} S/m and 259×10^{-6} S/m for *E. coli* strain 5K. These conductivities are expected to vary significantly between strains of bacteria based on their chemical makeup and protein expression profiles. Castellarnau et al. found that these values may vary by up to

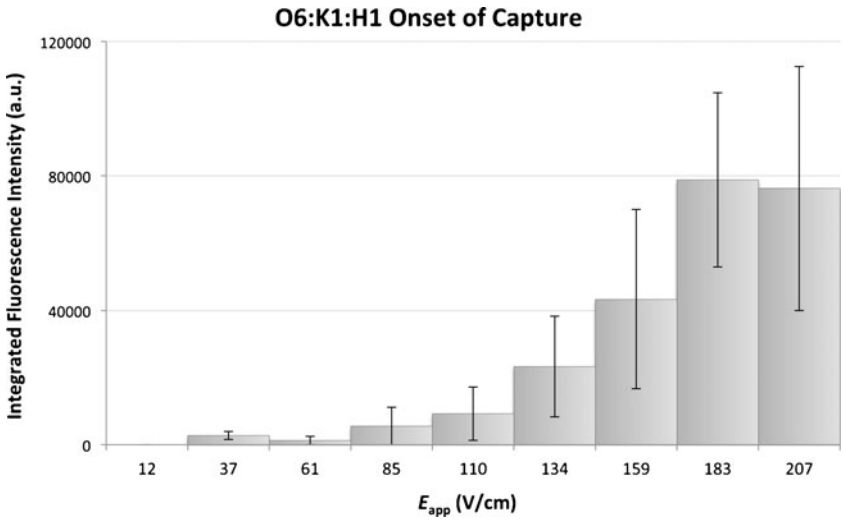

Fig. 5 Plot showing FI intensity versus applied field strength for five different preparations of serotype O6:K1:H1, each captured on a separate device

70 % for isogenic mutants of a single strain. Their experiments demonstrated that isogenic mutants of *E. coli*, differing at one allele, express sufficiently divergent phenotypes for different dielectrophoretic behavior.

Discussions of bacterial dielectric properties typically stop short of assigning or estimating specific values for μ_{DEP}. An experimental value of μ_{DEP} can be deduced from g-iDEP data by observing that the electrokinetic (F_{EK}) and dielectrophoretic forces (F_{DEP}) balance at the noted gate for the appropriate E_{onset}. This estimation was only calculated for the serovar that was captured at all three gates, O6:K1:H1, and resulted in a value of $-1.4\pm0.9 \times 10^{-17}$ m^4/V^2 s—a reasonable value compared to other particles measured in insulator dielectrophoretic systems (polystyrene, 1 μm, -2×10^{-16} m^4/V^2 s) [36]. This mobility can be used along with the local electric field strength to estimate the magnitude of the focusing forces exerted upon a single captured bacterium. For E_{onset} at a 27-μm gate, COMSOL Multiphysics modeling indicated centerline values of $\nabla|E|^2$ were approximately 1.0×10^{15} V^2/m^3. For this calculation, an *E. coli* cell was treated as a prolate ellipsoid with major axis $a=2$ μm and minor axis $b=0.5$ μm. Using these assumptions and calculated values, the force is approximately 0.2 nN ($F_{EK} \leq -F_{DEP} = 2 \times 10^{-10}$ N).

The general features of the observed capture of *E. coli* in a sawtooth g-iDEP device are consistent with previous results obtained using cells and other bioparticles. The characteristic behaviors have been described in detail elsewhere [27]. Briefly, the insulating PDMS constrictions yield intense electric field gradients. As particles approach a gate, they experience increasing dielectrophoretic force, which

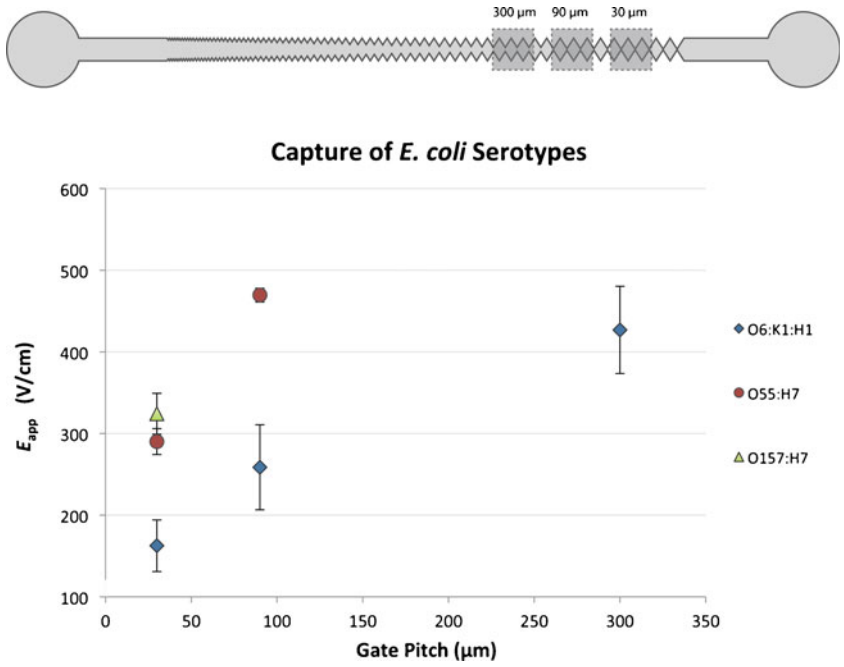

Fig. 6 Plot showing onset field required for capture for all three serotypes of *E. coli*, at three different gate pitches (27, 90, and 300 μm). Onset field differs for all three serotypes, indicating that they can be differentiated based on their electrokinetic behavior within a g-iDEP device. The data marker hides error bars for O55:H7 at the 90-μm gates

approaches a local maximum value. Negative DEP force is directed away from these regions, thus maximally opposing net EK force just before a particle passes the center of a gate. The magnitude of local electric field strength is proportional to E_{app} and inversely proportional to cross-sectional area. Thus local magnitudes of $\nabla|E|^2$ and resulting DEP force are a function of both E_{app} and gate pitch. Trapping occurs when DEP force exerted on a particle exceeds net EK force.

The dependence of capture on E_{app} and gate pitch was observed for all three serotypes (Fig. 6). A difference in E_{app} required for capture at a given gate between any two particle types indicates that they possess either differing μ_{EK}, μ_{DEP}, or both. A sufficient difference in these factors indicates that two particles could be differentiated.

When E_{app} was less than 100 V/cm, dielectrophoretic force was insufficient for capture of any cells. Capture at field strengths less than this value would require either a smaller gate pitch or a reduction in EK velocity. The latter could potentially be achieved by a reduction in EOF. Values of E_{app} above approximately 730 V/cm were unattainable due to equipment constraints. This represents the maximum potential of 3,000 V that could be applied to the channel using the existing power supply. Application of higher potentials is also impractical due to excessive Joule heating, which causes bubble formation within the channel, particularly where a large potential drop occurs across narrow gates.

Variables that could not be precisely controlled or quantitated, such as bacterial cell count, staining efficiency, pressure-driven and electroosmotic flow control, slightly varying properties for the individual cells, and photobleaching effects all contribute to the overall variance.

All samples were inspected at relatively high magnification before and after collection to observe the typical swimming and tumbling behaviors characteristic of the serotype. In all cases investigated, similar behaviors were observed for both conditions, suggesting that the high electric field and possible Joule heating did not negatively impact the bacteria in a significant manner. This is attributed to the relatively weak external field strength compared to local zeta potential/lipid bilayer field strength, which are typically several orders of magnitude higher than those estimated to be present within these devices.

These results show that O157:H7, O55:H7, and O6:K1:H1 serotypes of *E. coli* can be differentiated using g-iDEP operated with DC fields. In different pathogenic and non-pathogenic *E. coli* serotypes, small differences in cell structure, membrane, and wall composition are shown to be sufficient for differentiating populations. Current literature sources offer scant quantitative data regarding physical and electrical differences between strains of *E. coli*. Strain-to-strain variations in mean size or geometry are unknown. If such variation existed, however, it could be expected to contribute significantly to differences in both electrophoretic and dielectrophoretic force. Strain-specific differences in the biochemical makeup of the cell membrane and wall are likely to affect bacterial surface charge and conductivity. These parameters will in turn yield characteristic differences in electrophoretic and dielectrophoretic force.

Although it has not been demonstrated here, it is plausible that simultaneous separation and capture of all three serotypes within a single channel is achievable. This supports the idea that this approach can be adapted for future separation and identification of similar bacteria in microfluidic devices. However, this would require restructuring the progression of gate pitch along the channel. Future efforts will evaluate the implementation and efficiency of such separations. Specifically, advancements in channel geometry and surface treatments, along with the possible use of DC offset AC fields, promise to extend the abilities and applicability of this approach.

While the work presented here must adapt to the semantics of existing microbiological methods, the mechanism of identification and differentiation pursued here differs. Large-scale, phenotypic differences arise from molecular origins, which are concomitantly associated with identifiable and characteristic variation of cellular electric properties. With sufficient separatory resolution, gradient insulator-based dielectrophoresis (g-iDEP) will enable separation of many if not all of the categories currently used by microbiologists.

Conclusion

Using a g-iDEP strategy implemented with a pattern of sawtooth insulators has demonstrated differentiation of three serotypes of *E. coli* bacteria. While previous work has shown differentiation of bacteria based on species or live/dead state, this is the first demonstration of serotype differentiation using DC fields or insulator-based dielectrophoresis. Capture behavior was consistent with electric field modeling and overlapped with capture zones predicted from negative DEP forces. The results presented here indicate that all three serotypes could be discretely captured within a single separatory channel. Further modeling and design will facilitate optimization of g-iDEP channel geometry for the separation and capture of similar bioanalytes from complex mixtures. Such improvements will aid the development of new bioanalytical tools that enable the identification of microbes through precise and rapid separations.

References

1. Whitman WB, Coleman DC, Wiebe WJ (1998) Prokaryotes: the unseen majority. Proc Natl Acad Sci U S A 95(12):6578–6583. doi: 10.1073/pnas.95.12.6578

2. Hooper LV, Gordon JI (2001) Commensal host–bacterial relationships in the gut. Science 292(5519):1115–1118. doi:10.1126/science.1058709
3. Agata EMCD, Gautam S, Green WK, Tang Y-W (2002) High rate of false-negative results of the rectal swab culture method in detection of gastrointestinal colonization with vancomycin-resistant enterococci. Clin Infect Dis 34(2):167–172. doi:10.1086/338234
4. Benjamin RJ, Wagner SJ (2007) The residual risk of sepsis: modeling the effect of concentration on bacterial detection in two-bottle culture systems and an estimation of false-negative culture rates. Transfusion 47(8):1381–1389. doi:10.1111/j.1537-2995.2007.01326.x
5. Scallan E, Griffin PM, Angulo FJ, Tauxe RV, Hoekstra RM (2011) Foodborne illness acquired in the United States—unspecified agents. Emerg Infect Dis 17(1):16–22
6. Black JG (1996) Microbiology: principles and applications. Prentice Hall, Upper Saddle River
7. Tenover FC (2010) Potential impact of rapid diagnostic tests on improving antimicrobial use. In: Bush K (ed) Antimicrobial therapeutics reviews, vol 1213. Annals of the New York Academy of Sciences, New York, pp 70–80. doi:10.1111/j.1749-6632.2010.05827.x
8. Suehiro J, Noutomi D, Shutou M, Hara M (2003) Selective detection of specific bacteria using dielectrophoretic impedance measurement method combined with an antigen–antibody reaction. J Electrost 58(3–4):229–246. doi:10.1016/s0304-3886(03)00062-7
9. Gascoyne PRC, Noshari J, Becker FF, Pethig R (1994) Use of dielectrophoretic collection spectra for characterizing differences between normal and cancerous cells. IEEE Trans Ind Appl 30(4): 829–834. doi:10.1109/28.297896
10. Huang Y, Wang XB, Becker FF, Gascoyne PRC (1996) Membrane changes associated with the temperature-sensitive P85(gag-mos)-dependent transformation of rat kidney cells as determined by dielectrophoresis and electrorotation. Biochim Biophys Acta Biomembr 1282(1):76–84
11. Becker FF, Wang XB, Huang Y, Pethig R, Vykoukal J, Gascoyne PRC (1994) The removal of human leukemia cells from blood using interdigitated microelectrodes. J Phys D-Appl Phys 27(12):2659–2662. doi:10.1088/0022-3727/27/12/030
12. Becker FF, Wang XB, Huang Y, Pethig R, Vykoukal J, Gascoyne PRC (1995) Separation of human breast-cancer cells from blood by differential dielectric affinity. Proc Natl Acad Sci U S A 92(3):860–864
13. Burt JPH, Pethig R, Gascoyne PRC, Becker FF (1990) Dielectrophoretic characterization of Friend murine erythroleukaemic cells as a measure of induced differentiation. Biochim Biophys Acta 1034(1):93–101
14. Wang XB, Huang Y, Gascoyne PRC, Becker FF, Holzel R, Pethig R (1994) Changes in Friend murine erythroleukemia cell membranes during induced differentiation determined by electrorotation. Biochim Biophys Acta Biomembr 1193(2):330–344
15. Petr J, Maier V (2012) Analysis of microorganisms by capillary electrophoresis. Trac Trends Anal Chem 31:9–22. doi:10.1016/j.trac.2011.07.013
16. Armstrong DW, Schulte G, Schneiderheinze JM, Westenberg DJ (1999) Separating microbes in the manner of molecules. 1. Capillary electrokinetic approaches. Anal Chem 71(24):5465–5469. doi:10.1021/ac990779z
17. Srivastava SK, Daggolu PR, Burgess SC, Minerick AR (2008) Dielectrophoretic characterization of erythrocytes: positive ABO blood types. Electrophoresis 29(24):5033–5046. doi:10.1002/elps.200800166
18. Chou CF, Tegenfeldt JO, Bakajin O, Chan SS, Cox EC, Darnton N, Duke T, Austin RH (2002) Electrodeless dielectrophoresis of single- and double-stranded DNA. Biophys J 83(4):2170–2179
19. Cummings E, Singh A (2003) Dielectrophoresis in microchips containing arrays of insulating posts: theoretical and experimental results. Anal Chem 75(18):4724–4731. doi:10.1021/ac0340612
20. Pysher MD, Hayes MA (2007) Electrophoretic and dielectrophoretic field gradient technique for separating bioparticles. Anal Chem 79(12):4552–4557. doi:10.1021/ac070534j
21. Mack C (2007) Fundamental principles of optical lithography: the science of microfabrication. Wiley, Chichester
22. Staton SJR, Jones PV, Ku G, Gilman SD, Kheterpal I, Hayes MA (2012) Manipulation and capture of A beta amyloid fibrils and monomers by DC insulator gradient dielectrophoresis (DC-iGDEP). Analyst 137(14):3227–3229. doi:10.1039/C2an35138b
23. Hsiao AP, Barbee KD, Huang X (2010) Microfluidic device for capture and isolation of single cells. Proc Soc Photo Opt Instrum Eng 7759:77590W_1. doi:10.1117/12.861563
24. Preira P, Grandne V, Forel JM, Gabriele S, Camara M, Theodoly O (2013) Passive circulating cell sorting by deformability using a microfluidic gradual filter. Lab Chip 13(1):161–170. doi:10.1039/c2lc40847c
25. Phillips JA, Xu Y, Xia Z, Fan ZH, Tan WH (2009) Enrichment of cancer cells using aptamers immobilized on a microfluidic channel. Anal Chem 81(3):1033–1039. doi:10.1021/ac802092j
26. Olitzki L (1932) Electric charge of bacterial antigens. J Immunol 22(4):251–256
27. Jones PV, Staton SJR, Hayes MA (2011) Blood cell capture in a sawtooth dielectrophoretic microchannel. Anal Bioanal Chem 401(7):2103–2111. doi:10.1007/S00216-011-5284-9
28. Chen KP, Pacheco JR, Hayes MA, Staton SJR (2009) Insulator-based dielectrophoretic separation of small particles in a sawtooth channel. Electrophoresis 30(9):1441–1448. doi:10.1002/elps.200800833
29. Hamadi F, Latrache H, Zahir H, Elghmari A, Timinouni M, Ellouali M (2008) The relation between *Escherichia coli* surface functional groups' composition and their physicochemical properties. Braz J Microbiol 39(1):10–15. doi:10.1590/s1517-83822008000100003
30. Amory DE, Mozes N, Hermesse MP, Leonard AJ, Rouxhet PG (1988) Chemical analysis of the surface of microorganisms by X-ray photoelectron spectroscopy. Fems Microbiol Lett 49(1):107–110. doi:10.1111/j.1574-6968.1988.tb02690.x
31. El Ghmari A, Latrache H, Hamadi F, El Louali M, El Bouadili A, Hakkou A, Bourlioux P (2002) Influence of surface cell structures on physicochemical properties of *Escherichia coli*. Microbiologica 25(2):173–178
32. Latrache H, Mozes N, Pelletier C, Bourlioux P (1994) Chemical and physicochemical properties of *Escherichia coli*: variations among three strains and influence of culture conditions. Colloids Surf B: Biointerfaces 2(1–3):47–56. doi:10.1016/0927-7765(94)80017-0
33. Lytle DA, Rice EW, Johnson CH, Fox KR (1999) Electrophoretic mobilities of *Escherichia coli* O157: H7 and wild-type *Escherichia coli* strains. Appl Environ Microbiol 65(7):3222–3225
34. Pethig R (2010) Dielectrophoresis: status of the theory, technology, and applications (vol 4, 022811, 2010). Biomicrofluidics 4 (3). doi:10.1063/1.3474458
35. Castellarnau M, Errachid A, Madrid C, Juarez A, Samitier J (2006) Dielectrophoresis as a tool to characterize and differentiate isogenic mutants of *Escherichia coli*. Biophys J 91(10):3937–3945. doi:10.1526/biophysj.106.088534
36. Weiss NG, Jones PV, Mahanti P, Chen KP, Taylor TJ, Hayes MA (2011) Dielectrophoretic mobility determination in DC insulator-based dielectrophoresis. Electrophoresis 32(17):2292–2297. doi:10.1002/Elps.201100034